NANO LETTERS

2008
Vol. 8, No. 2
700−705

Controlled Growth of Super-Aligned Carbon Nanotube Arrays for Spinning Continuous Unidirectional Sheets with Tunable Physical Properties

Kai Liu,[†,‡] Yinghui Sun,[†] Lei Chen,[†] Chen Feng,[†,‡] Xiaofeng Feng,[†,‡] Kaili Jiang,*[,†,‡] Yonggang Zhao,*[,†] and Shoushan Fan[†,‡]

Department of Physics, Tsinghua-Foxconn Nanotechnology Research Center, Tsinghua University, Beijing 100084, China

Received September 10, 2007; Revised Manuscript Received December 10, 2007

ABSTRACT

We report controlled syntheses of super-aligned carbon nanotube (CNT) arrays with the desired tube-diameter, number of walls, and length for spinning continuous unidirectional sheets to meet a variety of industrial demands. The tube-diameter distribution of super-aligned arrays is well controlled by varying the thicknesses of catalyst films, and the length of them is tuned by the growth time. Further investigation indicates that the physical properties of the unidirectional sheets, such as electrical transport, optical transmittance, and light emission properties, can be well tuned by the tube-diameter- and length-controlled growth. This work extends the understanding of the super-aligned CNT arrays and will be very helpful in developing further applications.

Super-aligned carbon nanotube (CNT) arrays are distinguished from ordinary vertically aligned CNT arrays by their "super-aligned" nature, that is, the CNTs in super-aligned arrays have a much better alignment than those in ordinary arrays (Figure 1), which is a consequence of the narrower diameter distribution and higher nucleation density.[1,2] The key feature of a super-aligned CNT array is that continuous unidirectional sheets, composed of a thin layer of parallelly aligned pure CNTs, can be directly drawn from it in solid state.[1−6] The prerequisite for these vertically aligned CNTs to transform into horizontally aligned thin films is that the CNTs in super-aligned arrays have very clean surfaces and thus very strong van der Waals interactions with neighboring CNTs.[2] The as-produced sheets are transparent and highly conductive, which is also distinguished from random CNT films by their "unidirectional" nature, that is, CNTs in it are parallelly aligned in the draw direction and end-to-end jointed forming continuous thin films. Many potential applications for these have been demonstrated, for example as polarizers, transparent conducting films (TCFs), and polarized light sources, etc.[1,4] After passing through volatile solutions[2] or being twisted,[3,6] the sheets can further condense into shrunk yarns. These shrunk yarns have high tensile strengths and Young's moduli,[2,3,6] and are good candidates for thermionic[7] and field emission[8] electron sources. There is no doubt that more and more applications of unidirectional CNT sheets will be demonstrated in the future.

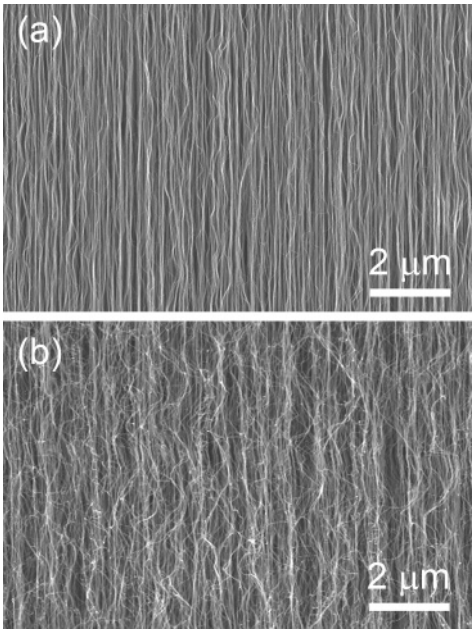

Figure 1. Comparison of super-aligned and ordinary arrays. (a) SEM side-view image of a super-aligned CNT array. (b) SEM side-view image of an ordinary CNT array.

* Corresponding authors. E-mail: (K.J.) jiangkl@tsinghua.edu.cn; (Y.Z.) ygzhao@tsinghua.edu.cn.
[†] Department of Physics.
[‡] Tsinghua-Foxconn Nanotechnology Research Center.

10.1021/nl0723073 CCC: $40.75
Published on Web 02/13/2008

However, to realize large-scale applications of unidirectional CNT sheets, there are two challenges in this field. The first challenge is how to scale up the synthesis, including enlarging the area of arrays and achieving batch growth. In 2005, we successfully synthesized super-aligned CNT arrays on 4 in. silicon wafers in low-pressure chemical vapor deposition (LP-CVD) systems.[2] One wafer of super-aligned CNTs is capable of being transformed into a continuous unidirectional CNT sheets which is 10 cm wide and 100 m long. Recently we have also achieved batch growth of super-aligned CNT arrays on 4 in. wafers in a 6 in. LP-CVD system. Despite these achievements, one fact remains to date: the only synthesized super-aligned CNTs suitable for drawing sheets with are multiwalled CNTs (MWCNTs) with a relatively large tube-diameter of 10∼15 nm.[1−6] However, sheets composed of small diameter CNTs, such as few-walled, double-walled, and single-walled CNT (abbreviated as FWCNT, DWCNT, SWCNT, respectively), possess some unique properties that are much more desirable in future industrial applications such as thin film transistors. Therefore, the second challenge is how to achieve controlled syntheses of super-aligned CNT arrays with the desired tube-diameter, number of walls, and length to meet a variety of industrial demands.

In this letter, we present our progress in tuning the physical properties of as-produced unidirectional CNT sheets by controlling the tube-diameter and the length of super-aligned CNT arrays. By controlling the thickness of catalyst films from 0.2 to 5.0 nm (by quartz crystal thickness monitoring), the tube-diameter of super-aligned CNTs can be tuned from 6.2 nm (3∼4 walls) to 9.2 nm (6∼9 walls). The length of super-aligned CNT arrays can be easily altered by the growth time with the longest arrays reaching 900 μm. We then investigated the physical properties of unidirectional CNT sheets drawn from CNT arrays with different tube-diameters and lengths. The sheet resistance shows negative temperature dependence. This dependence is more prominent with the reduction of tube-diameter and fits well with the three-dimensional hopping model. The sheet resistivity, the optical transmittance, and the degree of polarized light emission all decrease with increasing the length of CNT arrays, which may be ascribed to the bundling effect discussed below. These results indicate that the physical properties can be well tuned by controlled growth of super-aligned CNT arrays and will be helpful for further design of devices for applications.

Our super-aligned CNT arrays were synthesized in an atmospheric-pressure chemical vapor deposition (AP-CVD) tube furnace. The reactor consists of a 2.7 cm diameter quartz tube and a semi-opened quartz boat with an inlet (see Figure S1 in Supporting Information) that was convenient for controlled operations.[9−11] The substrates were SiO_2/Si wafers coated with thin Fe films deposited by electron beam (e-beam) evaporation. For the growth, the substrate was first placed inside the semi-opened quartz boat and then was heated up in the flowing argon gas (leading Ar through inlet II as labeled in Figure S1) to the growth temperature of 660∼680 °C for 15 min. Then H_2 and C_2H_2 were added to

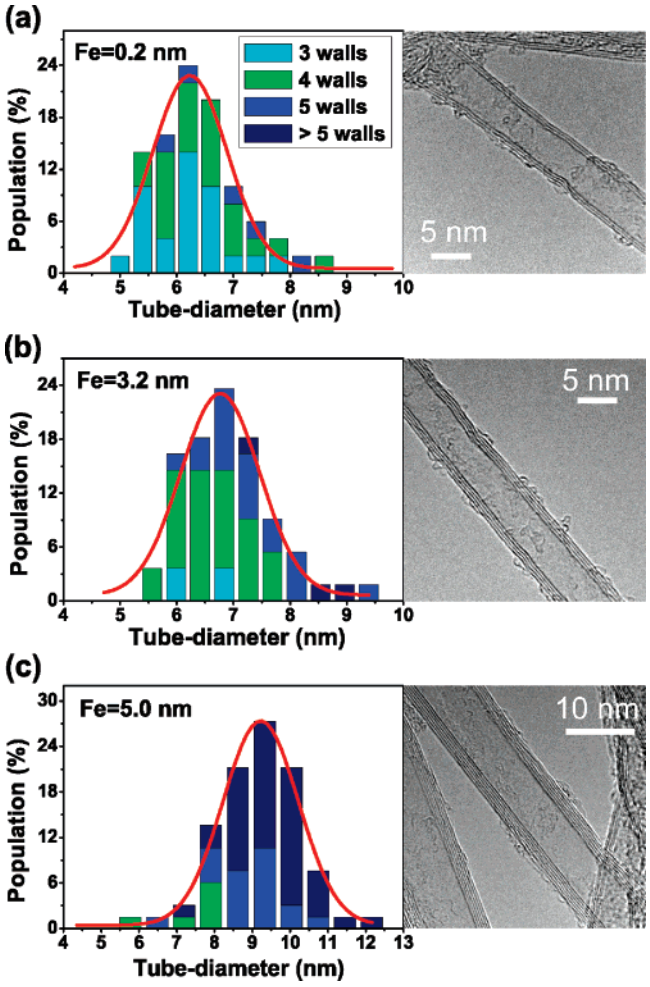

Figure 2. A family of TEM images and histograms showing the type and the tube-diameter of super-aligned CNT arrays synthesized on (a) 0.2 nm, (b) 3.2 nm, and (c) 5.0 nm thick Fe films with Gaussian fitting (red solid lines).

the Ar gas to start the growth of super-aligned CNT arrays. We found that the heating-up step in Ar was crucial for the formation of super-aligned CNT arrays. In contrast, we tried the heating-up step either in the flowing H_2 (leading H_2 through inlet II as labeled in Figure S1) or without flowing gas (holding in the static Ar ambience without leading any gas through inlet II as labeled in Figure S1), but the as-grown arrays could not make sheets well. Thus, the ambient gas has influenced the nucleation process of super-aligned CNT arrays dramatically. We also found it much easier to synthesize super-aligned CNT arrays with a wide range of thicknesses of Fe films and growth conditions in our semi-opened quartz boat, compared with the synthesis in a totally opened one. The main difference between these two cases is likely to be the local flow rate and flow pattern of the reaction gases caused by different geometry around the substrates. This therefore suggests that the local environment is also crucial for the formation of super-aligned CNT arrays, a similar result to the syntheses of normal arrays.[12]

Using this semi-opened quartz boat, we can derive super-aligned CNT arrays from Fe films with thicknesses of 0.2∼5.0 nm. Figure 2 shows the distributions of the tube-diameter and the number of walls of super-aligned CNT

arrays grown on three typical Fe films. The optimized growth condition was slightly different for the three film thicknesses, that is, $Ar/H_2/C_2H_2 = 200/100/30$ sccm at 680 °C, $Ar/H_2/C_2H_2 = 300/100/30$ sccm at 680 °C, and $Ar/H_2/C_2H_2 = 300/100/30$ sccm at 660 °C for the growth on the 0.2, 3.2, and 5.0 nm thick Fe films, respectively. As shown in Figure 2a−c, it is evident that the tube-diameter and the number of walls both increase with increasing the thickness of thin Fe films. The majority of the as-grown super-aligned CNT arrays comprises 3 or 4 walls (90% of the population) with a mean tube-diameter of 6.2 nm, 4 or 5 walls (87% of the population) with a mean tube-diameter of 6.8 nm, and ≥5 walls (91% of the population) with a mean tube-diameter of 9.2 nm, corresponding to the 0.2, 3.2, and 5.0 nm thick Fe films, respectively. The phase diagram for a certain thickness of Fe film highlights an empirically well-known fact that the number of walls of a CNT strongly depends on the tube-diameter, which indicates that a smaller tube tends to have fewer walls. It also implies that, to acquire super-aligned SWCNT or DWCNT arrays in the future, the thickness of Fe films should be further reduced.

To control the length of super-aligned CNT arrays, we altered the growth time. Figure 3a shows the CNT array length as a function of growth time. We found an appropriate growth time is necessary for the synthesis of a super-aligned CNT array. The optimum time is 3∼15 min for the growth on a 3.2 nm thick Fe film, while it is 3∼12.5 min for that on a 5.0 nm thick Fe film, corresponding to the array lengths of 175∼900 μm and 106∼357 μm, respectively. Figure 3b shows two unidirectional sheets produced from super-aligned arrays with the length of 318 μm (top) and 656 μm (bottom). A unidirectional sheet drawn from a longer super-aligned array appears more opaque than that drawn from a shorter one. The longest super-aligned CNT array is synthesized on the 3.2 nm thick Fe film for 15 min with the length of 900 μm (Figure 3c).

Here, it should be noted that elongating the growth time within the optimum growth time does not induce the change of the tube-diameter of CNTs. To show that, we compared the diameter of CNTs from two super-aligned arrays grown for 3 min (Figure 2b) and for 10 min (Supporting Information, Figure S2) on the 3.2 nm thick Fe film and found they have very little difference, which suggests that the diameter of CNTs remain unchanged with elongating the growth time. We can get the answer from the growth curves in Figure 3a. During the optimum time for the synthesis of super-aligned arrays, the length of arrays elongates linearly with increasing the growth time, indicating that CNTs keep growing stably on catalyst particles during this period and the catalyst particles do not fuse together. Therefore the tube-diameter remain unchanged with elongating the growth time.

By varying the tube-diameter, the number of walls and the length of super-aligned CNT arrays as mentioned above, we are able to tune the electrical and optical properties of as-produced unidirectional CNT sheets, which will further facilitate different applications such as transparent conducting films (TCFs) with different sets of transparency and resistivity.

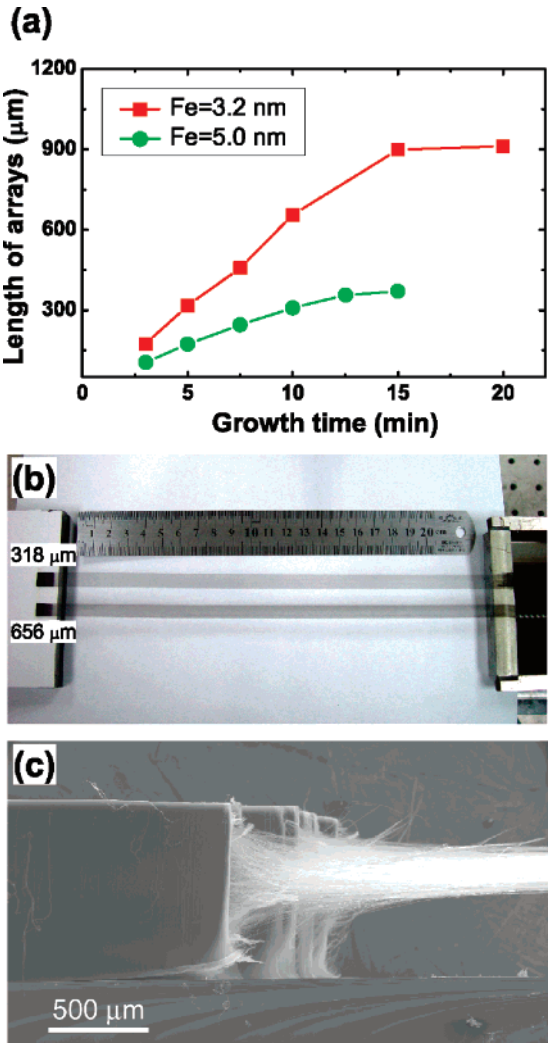

Figure 3. Evolution of length of arrays with time and the morphology of the as-grown super-aligned CNT arrays. (a) Length of arrays as a function of growth time for the syntheses on a 3.2 nm and a 5.0 nm thick Fe films. (b) Unidirectional sheets more than 20 cm long produced from 318 μm (upper) and 656 μm long (lower) super-aligned CNT arrays in top view. (c) Drawing a unidirectional sheet from a 900 μm long super-aligned CNT array in side view. The arrays in panels b and c were synthesized using the 3.2 nm thick Fe film.

We first measured the temperature dependence of the sheet resistance in the draw direction by the four-probe method. For the electrical measurement, four parallel Ti (10 nm)/Au (30 nm) electrodes were fabricated on a polished SiO_2/Si wafer by UV-lithography, e-beam evaporation, and lift-off processes. Then a CNT sheet drawn from an array was placed on the substrate with the CNTs aligned perpendicularly to the electrodes. Several ethanol drops were added onto the substrate to make sure the unidirectional CNT sheets attached tightly to the substrate. The ethanol-attaching method has advantages of both enhancing the adhesion force and avoiding the temperature discrepancy between the CNT sheet and the substrate. To obtain good electrical contacts, the contact points of CNT sheets and the electrodes were further reinforced by silver pastes. A typical structure for the four-probe measurement is shown in the inset of Figure 4a. The $R-T$ measurement was carried out in a liquid nitrogen

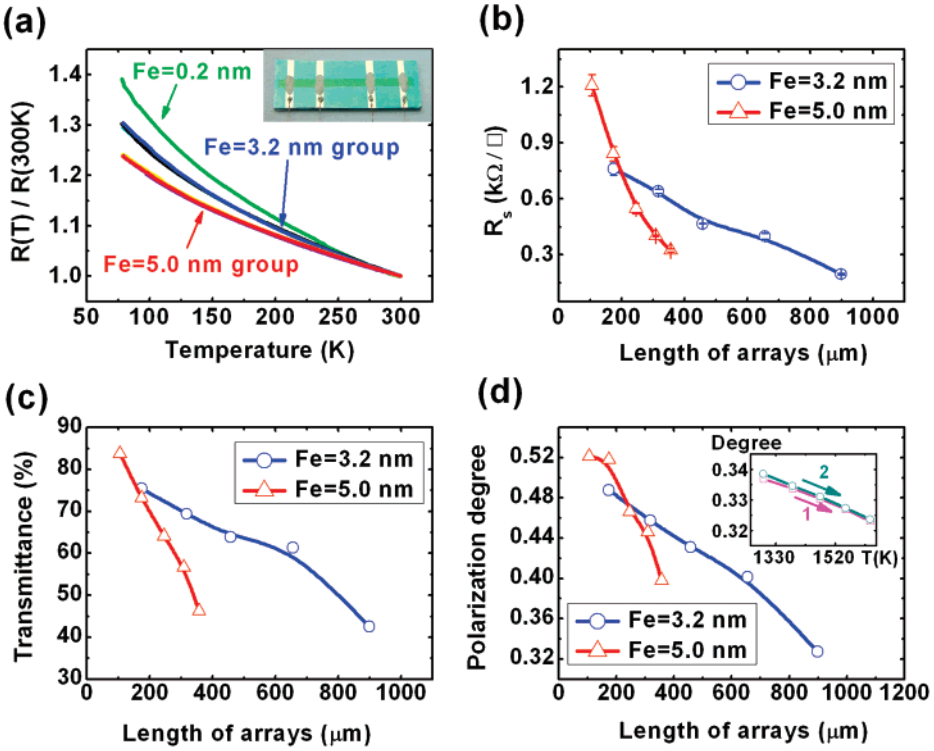

Figure 4. Electrical and optical properties. (a) Sheet resistance $R(T)$, normalized with respect to $R(300\ \mathrm{K})$, vs temperature. Note the three groups of curves. The upper green line is for the unidirectional sheets produced from a 250 μm long array grown on the 0.2 nm thick Fe film. The middle group of curves is for the sheets produced from arrays synthesized on a 3.2 nm thick Fe film with length 175 μm (cyan line), 318 μm (black line), and 656 μm (blue line). The bottom group is for the sheets derived from arrays with length 106 μm (yellow line), 174 μm (purple line), and 309 μm (red line) which are synthesized from a 5.0 nm thick Fe film. The inset shows a CNT sheet to be measured, which is tightly attached to the substrate with four parallel Ti/Au electrodes and further reinforced at the contact positions with the electrodes by silver pastes. (b) Sheet resistivity R_s vs array length at room temperature. Each data point and the corresponding error are calculated from the results of several sheet samples. The solid lines are eye guides. (c) Optical transmittance vs array length for the light with a wavelength of 550 nm. The optical transmittance of the full visible band for various array lengths are shown in Figure S5 in Supporting Information. (d) The polarization degree of light emissions from sheets that are produced from arrays with different lengths. The solid lines are eye guides. The inset is a two-cycle measurement of the degree of light emission polarization from low to high temperatures (labeled by "1" and "2" in sequence), which uses a CNT sheet produced from a 900 μm long array synthesized on the 3.2 nm thick Fe film.

cryostat with a cooling rate of 4 K/min. Figure 4a shows the curves of the normalized sheet resistance versus temperature. The different thicknesses of Fe films used in the CVD syntheses seem to result in the distinct groups of curves. The CNT sheet derived from a thinner Fe film has a larger temperature dependence of normalized sheet resistance, indicating that the resistance of a unidirectional CNT sheets with smaller tube-diameter and fewer walls tends to be more sensitive to the temperature. From 300 to 77 K, the CNT sheet resistance increases by about 40% for the 0.2 nm thick Fe film, about 30% for the 3.2 nm thick Fe film, and about 25% for the 5.0 nm thick Fe film. The negative temperature dependence of sheet resistance obeys the three-dimensional variable range hopping mechanism, following the equation $R = R_0 T^{1/2} \exp(T_0/T)^{1/4}$ (Supporting Information, Figure S4), similar to the electrical conduction behavior of twisted yarns.[13] In addition, as shown in the middle and bottom groups of curves in Figure 4a, the temperature dependence of the normalized resistance is not in turn heavily dependent on the length of arrays synthesized from a given film. This result indicates that the temperature dependence of normalized sheet resistance is very stable and not sensitive to the array length, which is crucial in real-world applications, where small variations between samples must not prevent stable performance.

One of the important applications of the unidirectional CNT sheets is TCF.[4] It is desirable to tune the transparency and resistivity of the sheets to meet different requirements of TCFs. Here, we show that both the transparency and resistivity can be easily tuned by controlling the diameter and length of super-aligned CNT arrays. We thus measured the sheet resistivity along the draw direction and the optical transmittance of suspended CNT sheets at room temperature. Here the sheet resistivity R_s is defined as RW/L, where R is the measured sheet resistance, W is the sheet width, and L is the sheet length. R_s indicates the sheet resistance per square in the sheet plane. As shown in Figure 4b,c and Figure S5 (Supporting Information), the sheet resistivity R_s and the optical transmittance show the same trend; they both reduce with increasing array length. R_s monotonically changes from 0.76 to 0.20 kΩ per square and the transmittance for the 550 nm wavelength light reduces from 76 to 44% when the length of arrays derived from 3.2 nm thick Fe film increases from 175 to 900 μm. The data for the 5.0 nm thick Fe film are from 1.21 to 0.32 kΩ per square and from 84 to 48% when the length of arrays increases from 106 to 357 μm.

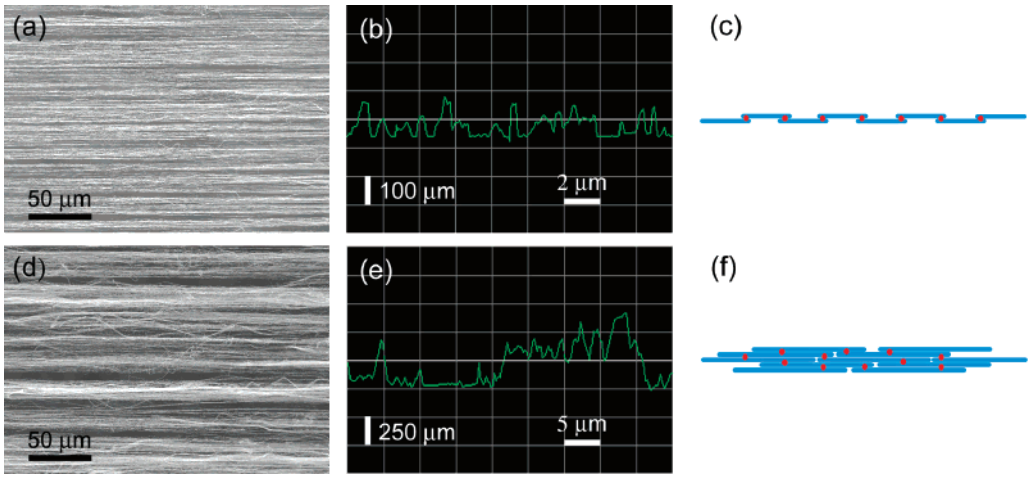

Figure 5. The morphology of the sheets produced from 175 μm (a,b) and 900 μm (d,e) long arrays grown from 3.2 nm thick Fe film and illustrations of the drawing process from short (c) and long (f) arrays. (a,d) SEM images of the sheets. (b,e) AFM height scan curves along the direction perpendicular to the draw direction. The cyan lines in panels c and f represent the bundles formed in arrays. They should be in the same size in spite of different array lengths. The red points in panels c and f represent the reassembling positions as mentioned in the text. Due to having much more reassembling positions, bundles in longer arrays will be in contact with more adjacent bundles to form larger bundles in the sheet.

The monotonic dependence of the sheet resistivity and the optical transmittance on the length of arrays provides a referenced basic data for the design of transparent conducting films.

Another promising optical application of sheets is as a stable planar source of polarized light. The polarized light emission is induced by electrons moving along the unidirectional one-dimensional CNTs in the sheets.[14] To study the light emission polarization, we applied a voltage to the two sides of a suspended sheet in the draw direction and used an optical spectrometer (wavelength 400∼800 nm) to measure the spectrum and the luminance. The wavelength dependence of spectral radiance fits the functional form of blackbody radiation from which the sheet temperature can be obtained.[14] The degree of light emission polarization is calculated from the luminance in directions parallel and perpendicular to the draw direction of the sheet. As shown in the inset of Figure 4d, we observe that the degree of polarization reduces with increasing sheet temperature, especially for sheets produced from long arrays, which is different from Zhang's result.[4] We also observe that the degree of polarization is stable at a fixed temperature. For a two-cycle measurement from 1300 to 1650 K, as labeled by "1" and "2" in sequence in the inset of Figure 4d, the results are nearly the same and highly repeatable. This excludes the possibility that CNTs are fused together to form larger ones at high temperatures and thus reduce the degree of polarization. The real reason for the polarization's dependence on temperature may be ascribed to the shift to short wavelengths for blackbody radiation due to high temperatures. In our experiment, the luminance is measured by the optical spectrometer in a wavelength span of 400∼800 nm. We observe that the polarization degree for a specific shorter wavelength is smaller, which is also observed by Zhang et al.[4] At high temperatures, the ratio of short to long wavelengths increases, and accordingly the degree of polarization reduces. In our measurements, the sheet produced from the longest array (900 μm) gives the greatest reduction in the degree of polarization, about 4% from 1290 to 1630 K.

The temperature dependence mentioned above prompted us to take the average of the measured data over a small temperature span (1200∼1650 K). Figure 4d shows the results for the sheets produced from the arrays with various lengths. The degree of polarization reduces with increasing array length, and the reduction rate is much larger for the sheets derived from the 5.0 nm thick Fe film arrays. These results are very similar to the trends of sheet resistivity and transmittance versus the array length as mentioned above, implying that there may be the same factor dominating the array length dependence of sheet resistivity, transmittance, and polarization degree.

The amorphous carbon on CNTs and the CNT surface density in arrays are possible factors which may affect the electrical and optical properties of the as-produced sheets. To estimate their values, we carried out the thermal gravimetric analysis (TGA) for the three types of super-aligned CNTs we studied. The results are shown in Figure S3 in Supporting Information. We found that the amount of amorphous carbon is very little and can be ignored in our samples. The surface density can be estimated from the mass loss to be about 5×10^{10}, 1×10^{11}, and 2.5×10^{10} tubes/cm^2 for the Fe = 0.2, 3.2, and 5.0 nm group, respectively. The surface density is largely determined by the nucleation density of CNTs, which is further determined by both the catalyst films and the growth conditions including gas rates and temperatures, but should not be relevant to the growth time. Therefore it will not affect the changes of electrical and optical properties with varying the array length.

As implied by the optical transmittance in Figure 4c, a sheet produced from a longer array appears to be thicker. To investigate this phenomenon, we compare two sheets produced from arrays with different lengths, as shown in Figure 5. Scanning electron microscopy (SEM) images in

Figure 5a,d indicate that the sheets consist of many horizontally aligned bundled CNTs. However, much larger bundles are formed in a sheet produced from a longer array (Figure 5d) in sharp contrast to that produced from a shorter one (Figure 5a). To further compare the thicknesses of these two kinds of sheets, we use atomic force microscopy (AFM) to scan the densified ones that are tightly attached to SiO_2/Si wafers by ethanol as mentioned above. The results are shown in Figure 5b,d. It is evident that the surface fluctuation is ~120 nm for a sheet produced from the 175 μm long array and ~500 nm for a sheet produced from the 900 μm long array. The larger fluctuation indicates a sheet produced from a longer array is much thicker and thus consists of more CNTs, leading to a lower resistivity and a lower transmittance.

In a large CNT bundle, a huge number of intertube contact points will form between adjacent CNTs, providing extra intertube paths for electron transport. Previous study in our group has shown that, due to increasing the number of contact points, the shrunk yarns have a much lower resistance compared to the unshrunk sheets.[15] Electron transport at these contact points gives rise to random directions of electric field of radiation, which breaks the polarization induced by the electron transport along CNTs and thus reduces the polarization degree. This effect is further shown by the fact that a yarn shrunk from a sheet by volatile solutions stops polarized emission totally. As mentioned above, a sheet produced from a longer array consists of larger CNT bundles. It thus has many more intertube contact points and as a result a lower polarization degree of light emission.

The question is why CNTs in the sheet produced from longer arrays tend to form larger bundles. If CNTs joint end-to-end while drawing,[2] then the mean bundle size for various array lengths should be not much different under the same set of growth conditions. In fact, however, the bundle structure in the super-aligned arrays is not fixed. Some small CNT groups depart from one bundle and join another adjacent bundle (indicated by the arrows in Figure S6 in Supporting Information and also shown in Figure 1b of ref 2), bridging and binding the adjacent bundles. This bundle-reassembling effect reveals that CNT bundles in super-aligned arrays can be jointed to each other throughout the whole inside of the arrays rather than merely at the end points. This can be further shown by the fact that if we use O_2 plasma to reduce the length of a super-aligned array and thus remove a layer of CNTs, the array can still give rise to unidirectional sheets well. However, a longer bundle in a longer array will have many more reassembling positions. When they are being drawn from the array, adjacent CNT bundles, connecting with each other through the reassembling positions, will be tensioned together to form a sheet. In this case, longer bundles from the longer arrays will bind more adjacent bundles, forming the larger bundles in the sheet, as shown by comparison of Figure 5 panel c versus panel f.

To summarize, we have been able to control the tube-diameter and the length of super-aligned CNT arrays and, as a result, to tune the physical properties of as-produced unidirectional sheets. The tube-diameter distribution of super-aligned arrays is well controlled by varying the thickness of catalyst films and optimizing the growth conditions, and the length of them is altered by the growth time. We further investigated the electrical and the optical properties of as-produced sheets, which are highly affected by the tube-diameter or the length of arrays. A new model describing the drawing process is proposed to explain the fact that a sheet produced from a longer array consists of larger bundles, which causes a reduction of sheet resistivity, transmittance, and polarization degree with increasing array length. The controlled syntheses and the above findings extend the understanding of super-aligned CNT arrays and will be very helpful in developing further applications.

Acknowledgment. The work was supported by the National Basic Research Program of China (2005CB623606) and NSFC (10704044, 10721404). We thank Tengge Ma and Mo Chen for the help in depositing Fe catalyst films and Sam Roots for proofreading.

Supporting Information Available: Illustration of experimental setup, tube-diameter histogram of one sample, TGA curves, fitting curves of electrical conduction, transmittance curves for the visible band, and a typical SEM image of the super-aligned CNT array. This material is available free of charge via the Internet at http://pubs.acs.org.

References

(1) Jiang, K. L.; Li, Q. Q.; Fan, S. S. *Nature* **2002**, *419*, 801.
(2) Zhang, X. B.; Jiang, K. L.; Feng, C.; Liu, P.; Zhang, L. N.; Kong, J.; Zhang, T. H.; Li, Q. Q.; Fan, S. S. *Adv. Mater.* **2006**, *18*, 1505.
(3) Zhang, M.; Atkinson, K. R.; Baughman, R. H. *Science* **2004**, *306*, 1358.
(4) Zhang, M.; Fang, S. L.; Zakhidov, A. A.; Lee, S. B.; Aliev, A. E.; Williams, C. D.; Atkinson, K. R.; Baughman, R. H. *Science* **2005**, *309*, 1215.
(5) Li, Q. W.; Zhang, X. F.; DePaula, R. F.; Zheng, L. X.; Zhao, Y. H.; Stan, L.; Holesinger, T. G.; Arendt, P. N.; Peterson, D. E.; Zhu, Y. T. *Adv. Mater.* **2006**, *18*, 3160.
(6) Zhang, X. F.; Li, Q. W.; Tu, Y.; Li, Y.; Coulter, J. Y.; Zheng, L. X.; Zhao, Y. H.; Jia, Q. X.; Peterson, D. E.; Zhu, Y. T. *Small* **2007**, *3*, 244.
(7) Liu, P.; Wei, Y.; Jiang, K. L.; Sun, Q.; Zhang, X. B.; Fan, S. S.; Zhang, S. F.; Ning, C. G.; Deng, J. K. *Phys. Rev. B.* **2006**, *73*, 235412.
(8) Wei, Y.; Weng, D.; Yang, Y. C.; Zhang, X. B.; Jiang, K. L.; Liu, L.; Fan, S. S. *Appl. Phys. Lett.* **2006**, *89*, 063101.
(9) Liu, K.; Jiang, K. L.; Feng, C.; Chen, Z.; Fan, S. S. *Carbon* **2005**, *43*, 2850.
(10) Liu, K.; Liu, P.; Jiang, K. L.; Fan, S. S. *Carbon* **2007**, *45*, 2379.
(11) Liu, K.; Jiang, K. L.; Wei, Y.; Ge, S. P.; Liu, P.; Fan, S. S. *Adv. Mater.* **2007**, *19*, 975.
(12) Fan, S. S.; Liang, W. J.; Dang, H. Y.; Franklin, N.; Tombler, T.; Chapline, M.; Dai, H. J. *Phys. E* **2000**, *8*, 179.
(13) Li, Q. W.; Li, Y.; Zhang, X. F.; Chikkannanavar, S. B.; Zhao, Y. H.; Dangelewicz, A. M.; Zheng, L. X.; Doorn, S. K.; Jia, Q. X.; Peterson, D. E.; Arendt, P. N.; Zhu, Y. T. *Adv. Mater.* **2007**, *19*, 3358.
(14) Li, P.; Jiang, K. L.; Liu, M.; Li, Q. Q.; Fan, S. S.; Sun, J. L. *Appl. Phys. Lett.* **2003**, *82*, 1763.
(15) Wei, Y.; Jiang, K. L.; Feng, X. F.; Liu, P.; Liu, L.; Fan, S. S. *Phys. Rev. B* **2007**, *76*, 045423.

NL0723073